arXiv:2009.11016v1 [cs.CV] 23 Sep 2020

Generative Model without Prior Distribution Matching

Cong Geng, Jia Wang, Li Chen, Zhiyong Gao
Shanghai Jiao Tong University
Institute of Image Communication and Network Engineering
Shanghai, China
{gengcong, jiawang, hilichen, zhiyong.gao}@sjtu.edu.cn

Abstract

Variational Autoencoder (VAE) and its variations are classic generative models by learning a low-dimensional latent representation to satisfy some prior distribution (*e.g.*, Gaussian distribution). Their advantages over GAN are that they can simultaneously generate high dimensional data and learn latent representations to reconstruct the inputs. However, it has been observed that a trade-off exists between reconstruction and generation since matching prior distribution may destroy the geometric structure of data manifold. To mitigate this problem, we propose to let the prior match the embedding distribution rather than imposing the latent variables to fit the prior. The embedding distribution is trained using a simple regularized autoencoder architecture which preserves the geometric structure to the maximum. Then an adversarial strategy is employed to achieve a latent mapping. We provide both theoretical and experimental support for the effectiveness of our method, which alleviates the contradiction between topological properties' preserving of data manifold and distribution matching in latent space.

Introduction

Generative models represent complex data distributions using a generator function that maps low-dimensional latent vectors subjected to a specified distribution to high-dimensional data outputs. Variational autoencoder (VAE) [Kingma and Welling 2014] and generative adversarial network (GAN) [Goodfellow et al. 2014] are two notable deep learning generative models. Compared with GAN, VAE has the benefit of an encoder that learns latent representation of data inputs, making VAE an effective tool for generating and understanding manifold structure in high-dimensional data. Traditional VAE and its variants are trained by minimizing a reconstruction error and a divergence to force the variational posterior to fit the prior. However, it's hard for the latent embedding to simultaneously keep the topological properties of the data manifold and satisfy a Gaussian distribution. It means the performance of VAEs is a trade-off between reconstruction and generation.

In this work, we present a generative model without prior distribution matching to solve the above trade-off. Different from VAEs which encourage the approximate posterior to match the prior, we propose a latent mapping letting the prior fit the embedding distribution. The key point of our method is the learning of the embedding distribution which is expected to preserve the structure of data manifold and is easy for the prior to learn. David Berthelot et al. [Berthelot et al. 2019] propose a regularization procedure that encourages interpolated outputs to appear more realistic using an adversarial learning strategy. It improves representation learning performance on downstream tasks. We extend this method to our embedding learning task and find it can help to capture the characteristics of embedding distribution. To avoid the learned embedding distribution to be over-dispersed, we introduce a batch normalization trick on the latent space based on the volume concentration of high dimensional sphere. After learning a useful latent representation, we employ a GAN structure to encourage the prior to match the embedding distribution. With our method, we can generate high dimensional data sampled from a specified prior while reconstructing observations from latent representations which preserve the topological properties of data manifolds. Overall, the main contributions of this work are as follows:

- We explain the causes of the existing trade-off in most variational based autoencoders and provide a theoretical analysis of our method on alleviating this trade-off problem.
- We introduce an autoencoder structure with an adversarial interpolation regularization and a batch normalization trick to obtain a learning-facilitated latent embedding representation that preserves the topological structure of the data manifold.
- We propose an adversarial based latent mapping in order to sample from a specified prior distribution when generating new high-dimensional data.

Related Work

Autoencoder (AE) networks [Vincent et al. 2010] are unsupervised approaches aiming at combining the reconstruction as well as the representation properties by learning an encoder-generator map. Since then, a lot of progress has been made based on autoencoders. These variants are generally divided into two categories: VAE-based and GAN-based. In the VAE-based case, AEs are regularized to explic-

Copyright © 2021, Association for the Advancement of Artificial Intelligence (www.aaai.org). All rights reserved.

itly match the distribution of the latent representations with a predefined prior. In the VAE-based case, VAE [Kingma and Welling 2014] introduces an additional loss into the reconstruction loss. This loss measures the KL divergence between the distribution of the latent representations and the prior. Along with learning continuous representations, vector-quantized VAE (VQVAE) [Oord, Vinyals, and Kavukcuoglu 2017] uses a vector quantization method allowing the model to circumvent issues of posterior collapse. In the GAN-based case, adversarial AE (AAE) [Makhzani et al. 2015] introduces an auxiliary subnetwork referred to as a discriminator based on the GAN framework and forces this discriminator to measure the difference between latent representations and the prior. Besides, Wasserstein autoencoder(WAE) [Tolstikhin et al. 2018] also employs MMD to measure the distribution divergence. Moreover, VAE-GAN [Larsen and Winther 2016] fuses both the VAE and GAN frameworks in the autoencoder which replaces the traditional pixel-wise reconstruction loss by an adversarial feature-wise reconstruction loss obtained from the GANs discriminator. Another famous integration for VAE and GAN is introVAE [Huang et al. 2018]. It requires no extra discriminators because the inference model itself serves as a discriminator to distinguish between the generated and real samples.

For latent representation, ACAI [Berthelot et al. 2019] proposes a regularization procedure which encourages interpolated outputs to appear more realistic by fooling a critic network which has been trained to recover the mixing coefficient from interpolated data. It demonstrates good interpolation can result in a useful representation which is more effective on downstream tasks. MI-AE [Qian et al. 2019] improves ACAI by introducing a multidimensional interpolation approach for each dimension of the latent representations and encouraging generated data points to be realistic in the GAN framework. Besides, S-VAE [Davidson et al. 2018, Xu and Durrett 2018] and SAE [Zhao, Zhu, and Zhang 2019] project latent variable on a sphere to improve learning on high-dimensional space. Other autoencoder techniques provide frameworks that attempt to shape the latent space with respect to factor disentanglement [Bouchacourt, Tomioka, and Nowozin 2017, Mathieu and Teh 2019].

Problem Definition

Notation. Throughout the paper, we use the following notations. We use calligraphic letters (*e.g.*, $\mathcal{X}$) to denote spaces, and bold lower case letters (*e.g.*, $\mathbf{x}$) to denote vectors. Let $p(x)$ be the real data distribution, and let $P_n{=}\{\mathbf{x}_i, \mathbf{y}_i\}_{i=1}^n{\in}\mathcal{X}{\times}\mathcal{Y}$ be the training data, where $\mathcal{X}$ denotes the data space.

Trade off in Variational Autoencoder

Traditional VAE models the distribution of observations $p_\theta(x)$ by specifying a prior $p(z)$ along with a likelihood $p_\theta(x|z)$ that connects it with the observation:

$$p_\theta(x) = \int p_\theta(x|z)p(z)dz \tag{1}$$

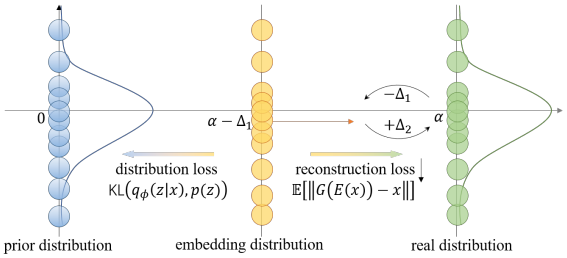

Figure 1: Intuitive understanding of Proposition 2

The integral for computing $p_\theta(x)$ is intractable, making it hard to maximize the marginal likelihood of the model under the data. To overcome this intractability, VAEs instead maximize the Evidence Lower Bound (ELBO) of the marginal likelihood:

$$\log p_\theta(x) \geq \mathbb{E}_{q_\phi(z|x)}[\log p_\theta(x|z)] - KL[q_\phi(z|x)||p(z)], \tag{2}$$

where $q_\phi(z|x)$ is the variational posterior. The neural networks used to parameterize $q_\phi(z|x)$ and $p_\theta(x|z)$ are referred to as the encoder and decoder, respectively. We can observe that the second term in ELBO, the Kullback-Leibler (KL) divergence captures how distinct the conditional distribution of latent representation corresponding to each training example is from the prior $p(z)$. The VAE objective minimizes KL divergence to force the encoder to output $\mu(x_i) = 0$ and $\sigma(x_i) = 1$ for all samples. In this case, the decoder will face an impossible task of reconstructing different samples from completely random noise which is called "posterior collapse". The following case will illustrate this phenomenon.

Proposition 1 *Assume $p(z)$ is some specified prior distribution. $p(x)$ is the real data distribution, if we let $KL[q_\phi(z|x)||p(z)] = 0$, for every $x \in \mathcal{X}$, then ELBO is globally optimized only if $p_\theta(x|z) = p(x)$ for every $z \in \mathcal{Z}$.*

Proposition 1 means VAE will completely lose reconstruction ability if we force $KL[q_\phi(z|x)||p(z)] = 0$. To avoid this, VAE requires manually fine-tuning the weight of the KL component and reconstruction hyper-parameters. In order to realize reconstruction, the variational posterior $q_\phi(z|x_i)$ is a Gaussian distribution whose mean and variance are related to the encoder and training sample x_i. That is,

$$q_\phi(z|x_i) \sim \mathcal{N}\big(\mu(x_i), \sigma(x_i)\big) \tag{3}$$

which is not guaranteeing that the overall encoded distribution $\mathbb{E}_{p(x)}[q_\phi(z|x)]$ matches $p(z)$. Figure 3 (a) shows the latent embedding trained by VAE. It illustrates this mismatching. The following example provides an extreme case to show that the KL divergence term is hard to be guaranteed if we incline to the reconstruction loss.

Proposition 2 *Suppose $\mathcal{X}, \mathcal{Z}$ are 1-D spaces. Assume $p(z)$ is some specified continuous prior distribution, $p(x)$ is a 1-D continuous distribution with finite support, $q_\phi(z|x)$ is continuous in finite support region for different x. then*

$$\sup_x KL[q_\phi(z|x)||p(z)] = +\infty, \tag{4}$$

when $\mathbb{E}_{p(x)}\big[\mathbb{E}_{q_\phi(z|x)}[logp_\theta(x|z)]\big]$ *achieves the maximum.*

Figure. 1 intuitively explains Proposition 2, which reveals that the KL divergence and the reconstruction loss may be hard to be guaranteed to be small simultaneously. To alleviate this problem, infoVAE [Zhao, Song, and Ermon 2019] introduces a mutual information term into original ELBO to weight the preference between correct inference and fitting the data distribution, and specify a preference on how much the model should rely on the latent variables:

$$\begin{aligned}\mathcal{L}_{\text{InfoVAE}} =& -\lambda KL[q_\phi(z)\|p(z)]- \\ & \mathbb{E}_{q(z)}\big[KL[q_\phi(x|z)\|p_\theta(x|z)]\big] + \alpha I_q(x;z) \\ \equiv& \mathbb{E}_{p(x)}\mathbb{E}_{q_\phi(z|x)}\left[\log p_\theta(x|z)\right] - \\ & (1-\alpha)\mathbb{E}_{p(x)}\big[KL[q_\phi(z \mid x)\|p(z)]\big]- \\ & (\alpha+\lambda-1)KL[q_\phi(z)\|p(z)]\end{aligned} \tag{5}$$

Essentially, infoVAE weights the KL term in original ELBO and adds another KL term $KL[q_\phi(z)\|p(z)]$ to further alleviate the contradiction between reconstruction and generation. When $\alpha = 1, \lambda = 1$, infoVAE can degenerate into AAE [Makhzani et al. 2015] which is equivalent to adding a mutual information term into the ELBO bound. WAE [Tolstikhin et al. 2018] minimizes the optimal transport cost $W_c\big(P_X; P_\theta(X)\big)$ based on the novel autoencoder formulation, leading to the following objective:

$$\begin{aligned}D_{WAE}\big(P_X; P_\theta(X)\big) = \inf_{Q_\phi(Z)} \mathbb{E}_{p(x)}\mathbb{E}_{q_\phi(z|x)}\big[c\big(x, G(z)\big)\big] \\ + \lambda \cdot D_Z\big(Q_\phi(Z), P_Z\big)\end{aligned} \tag{6}$$

WAE can be viewed as another version of AAE from the Wasserstein distance perspective. However, all these variants try to simultaneously achieve two conflicting goals: preserving the topological properties of data manifold and making sure that the latent codes provided to the decoder are informative enough to generate meaningful samples. In the actual training process, such autoencoders prone to get a trade-off between reconstruction and generation. The conflicting phenomenon is depicted in Fig. 3 (b).

Proposed Method

To solve the above problems, we expect to separate the two tasks of reconstruction and generation. Instead of imposing the latent representation match the prior, we let the prior fit the latent embedding distribution. For the purposes of optimization, we rewrite the reconstruction term in ELBO as follows:

$$\begin{aligned}&\mathbb{E}_{p(x)}\mathbb{E}_{q_\phi(z|x)}\left[\log p_\theta(x|z)\right] = \int q_\phi(z,x)\log p_\theta(x|z)dzdx \\ &= \int q_\phi(z,x)\log p_\theta(x,z)dzdx - \int q_\phi(z,x)\log p(z)dzdx \\ &= \int q_\phi(z,x)\log p_\theta(x,z)dzdx - \int q_\phi(z)\log p(z)dz\end{aligned} \tag{7}$$

Equation 7 can be transposed to:

$$\begin{aligned}\int q_\phi(z,x)\log p_\theta(x,z)dzdx = \mathbb{E}_{p(x)}\mathbb{E}_{q_\phi(z|x)}\left[\log p_\theta(x|z)\right] \\ + \int q_\phi(z)\log p(z)dz\end{aligned} \tag{8}$$

If we fix our encoder, equation 8 can obtain the maximum value when $q_\phi(z,x) = p_\theta(x,z)$. At this point, the two terms on the right respectively achieve the maximum. We need to impose $p_\theta(x|z) = q_\phi(x|z)$ and $p(z) = q_\phi(z)$. For a simple autoencoder, if we fix the encoder, it's flexible enough to find a decoder to satisfy $p_\theta(x|z) = q_\phi(x|z)$. Then we only need to make the prior match the embedding distribution, which is also not hard to achieve. There exists no trade-off in our framework between generation and reconstruction.

We introduce an extra generator g to match the latent embedding distribution from the prior. Then the decoder G maps latent samples $g(z)$ to data space $x = G(g(z))$. For implementation, we use the adversarial training to estimate the distance metric between distributions. Fig 2 shows our overall framework.

Autoencoder with an Adversarial Regularizer

The major challenge for our method is the determination of our latent representation. The latent space trained by autoencoder is expected to be concentrated and easy to learn for the prior. Therefore, inspired by ACAI [Berthelot et al. 2019] and MI-AE [Qian et al. 2019], we add an adversarial regularizer to the original autoencoder loss to improve our latent representation. Similar to ACAI, we use a discriminator d to form a GAN with our autoencoder to propel the linear interpolated data to perceptually approximate real data to as realistic an extent as possible. The objective of the discriminator can be reformulated as below:

$$\begin{aligned}L_{dis} =& \|d(x)\|^2 + \|d\big(\gamma x + (1-\gamma)\hat{x}\big) - \lambda\|^2 + \\ & \|d(x_\mu) - \mu - \lambda\|^2\end{aligned} \tag{9}$$

where, as above, $\hat{x}$ is the reconstruction of x through the autoencoder $\hat{x} = G(E(x))$, $x_\mu = G\big(\mu E(x_1) + (1-\mu)E(x_2)\big)$. λ and γ are two hyperparameters. μ is randomly sampled from the uniform distribution on [0, 0.5]. Different from ACAI and MI-AE, we constrain the discriminator's output of the interpolation between x and $\hat{x}$ to be the preset λ. Because we need to distinguish between the subtle difference between reconstruction data and real data to guide the encoder to obtain a better latent representation. Since the x_μ is less realistic than $\hat{x}$, we predict $\mu + \lambda$ for x_μ. With this loss function for discriminator, the autoencoders objective is modified by adding two regularization term:

$$L_{ae} = \|x - G(E(x))\|^2 + \omega_1\|d(x_\mu)\|^2 + \omega_2\|d(\hat{x})\|^2 \tag{10}$$

where ω_1, ω_2 are hyper-parameters for adjusting the weights of the above losses.

Latent Normalization

In high dimensional space, VAE suffers from the dimensional dilemma that can be interpreted via some counterintuitive geometric facts. The data examples for a dataset become rather sparse in high dimensions since the geometric

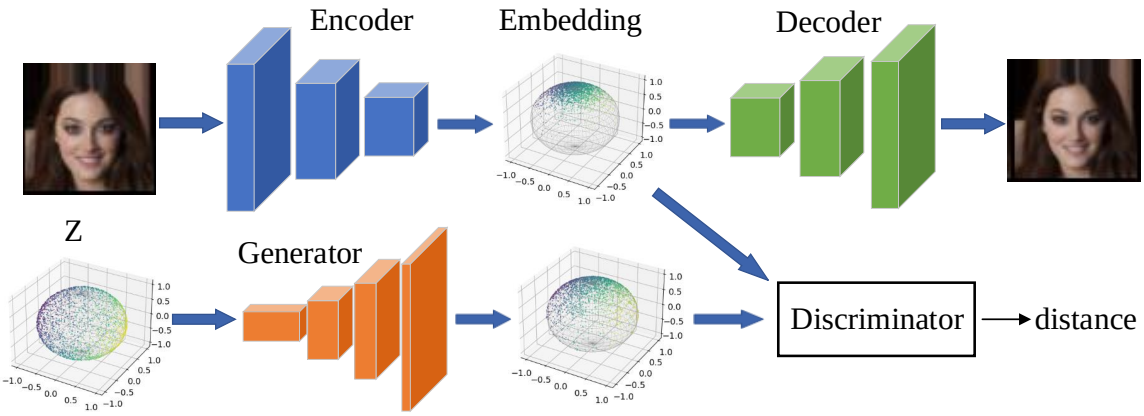

Figure 2: Overall Framework

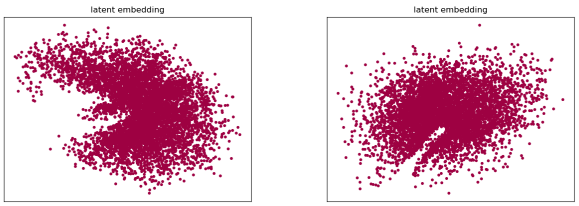

(a) VAE (b) AAE

Figure 3: The encoding results with different methods for digit "0" in MNIST Dataset.

property reveals that the volume ratio between a cube and its inscribed sphere goes to infinity when the dimension goes very large [van Handel 2014]. Therefore, it becomes challenging to fit a distribution in high dimensions. Based on these surprising phenomenons, we employ a simple batch normalization trick to make our embedding subjected to a distribution with its mean close to zero and variance to 1. This operation makes embedding distribution more concentrated and is easier for the prior to learn. The operation in the training process can be easily performed by:

$$x \overset{E}{\longmapsto} z \longmapsto BN(z) \longmapsto \hat{z} \overset{G}{\longmapsto} \hat{x} \tag{11}$$

In fact, this BN trick can be viewed as a spherical projection in high dimensional space since volume concentration [Blum, Hopcroft, and Kannan 2016] says that the volume of the sphere in the high-dimensional space is highly concentrated near the surface. The interior is nearly empty. The benefit of spherical projection over other latent regularization is that the 2-Wasserstein distance between two arbitrary sets of random variables randomly drawn on the sphere converges to a constant when the dimension is sufficiently large. Furthermore, Deli Zhao et al [Zhao, Zhu, and Zhang 2019] prove that the distance convergences to $\sqrt{2nr}$ where n is the number of the latent variables in the dataset and r is the sphere radius. This theorem illustrates the latent variables on the sphere are distribution-robust. However, It holds under a critical condition that latent vectors are randomly drawn from the sphere. Sometimes the condition violates if the prior and latent embedding are sampled from different orthants. Therefore, [Zhao, Zhu, and Zhang 2019] proposes a very simple approach by centralizing $z_i - \bar{z}_i \mathbf{1}$, where $z_i = [z_i^1, z_i^2, \cdots, z_i^{d_z}]$ and the mean $\bar{z}_i = \frac{1}{d_z}\sum_j z_i^j$. But this centralization will destroy the geometry of the latent embedding, which is against our original intention. Thanks to the BN operation, we can obtain a latent distribution with zero meanwhile preserving the geometric structure. After this latent normalization, we can guarantee that the distance between the prior and latent representation is small enough to alleviate the next latent mapping.

Latent Mapping

After getting the desired latent representation, we need to let the specified prior match this latent distribution. GAN based divergence estimation is widely applied in deep learning. Thus we introduce a GAN structure for our latent mapping. Specifically, we introduce a discriminator D in the latent space trying to separate $g(z)$ with z sampled from P_Z and latent embeddings $E(x)$ subject to $Q_\phi(Z)$. For network training, we employ the hinge version of the adversarial loss which were applied in SAGAN [Zhang et al. 2019] and BigGAN [Brock, Donahue, and Simonyan 2019], resulting in the following discriminator objective:

$$\begin{aligned} L_D = &\mathbb{E}_{x\sim p_r(x)}[relu(1 - D(E(x)))] + \\ &\mathbb{E}_{z\sim p(z)}[relu(1 + D(g(z)))] \end{aligned} \tag{12}$$

For generator g, the loss function can be written as follows:

$$L_g = \mathbb{E}_{z\sim p(z)}\big[-D(g(z))\big] \tag{13}$$

Experiments

In this section, we evaluate our method on toy datasets and two widely-used image datasets-MNIST [LeCun 1998] and CelebA [Liu et al. 2015]. As a preliminary evaluation, we use low-dimensional datasets Swiss-roll to visually justify

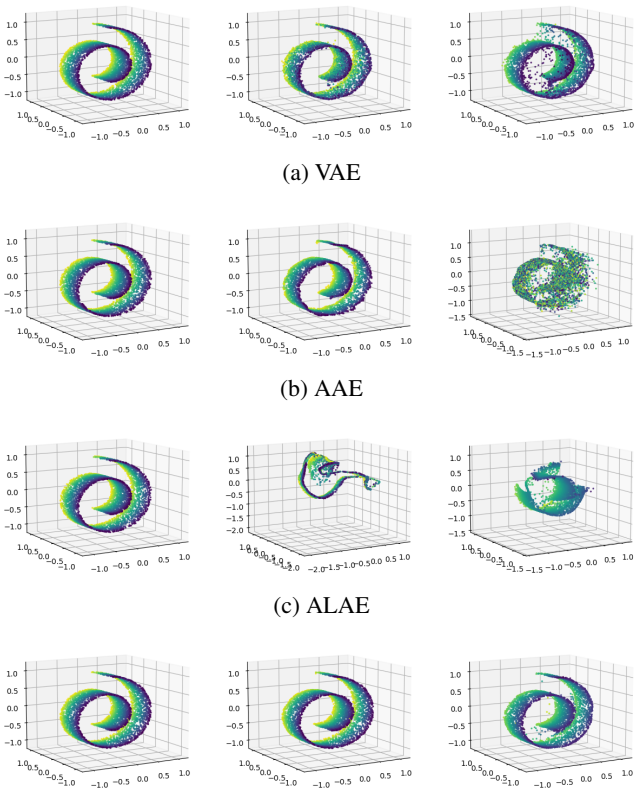

(a) VAE

(b) AAE

(c) ALAE

(d) Ours

Figure 4: The reconstructed and generated data manifolds for swiss-roll. The left column is the input manifold, the middle column is the reconstruction manifold, and the right column is the generated manifold from Gaussian prior.

that our learned latent embedding can preserve the topological properties of the data manifold and the prior can match our embedding distribution well, resulting in a satisfying reconstruction and generation simultaneously. Meanwhile, the two large scale datasets highlight a variety of challenges that our method should address and evaluation on them is adequate to support the advantages of ours.

Swiss-roll

We compare our method to the VAE [Kingma and Welling 2014], AAE [Makhzani et al. 2015], and ALAE [Pidhorskyi, Adjeroh, and Doretto 2020]. For each method, we apply the same architectures with our paper. We uniformly sample 5000 samples on swiss-roll as the data manifold and use a 2D unit Gaussian distribution as our prior. Figure 4 shows the reconstruction of the input data manifold and generated manifold with Gaussian samples as the input. Because of the reconstruction term in both VAE and AAE, they can get satisfying reconstructed manifolds. However, the generated manifolds are less satisfied due to the trade-off in their training. For ALAE, its principal training framework is based on GAN, not including a clear reconstruction loss. Therefore, ALAE fails to capture the topological structure of the original manifold even on generation task. Figure 5

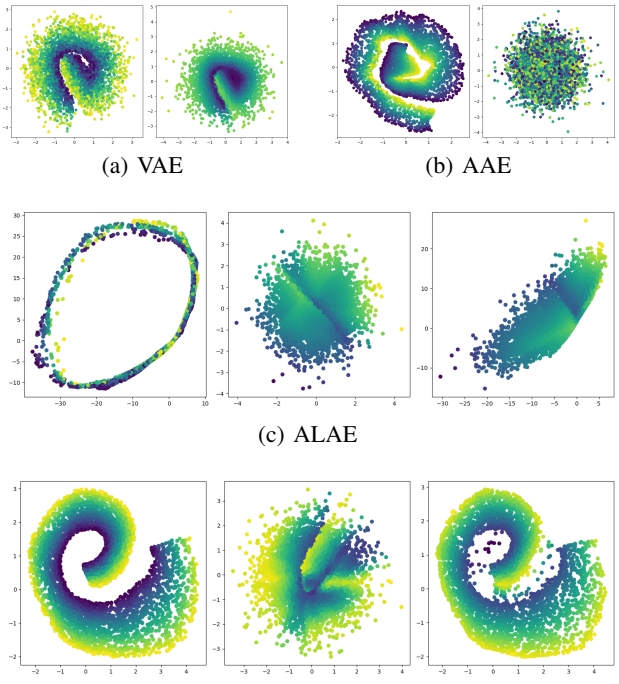

(a) VAE

(b) AAE

(c) ALAE

(d) Ours

Figure 5: Latent distributions for swiss-roll. The left image is the latent embedding, the middle image is the Gaussian prior. For ALAE and our method, the right image is the generated latent distribution from Gaussian prior.

further illustrates the relation between latent representation and prior distribution. The latent embedding for VAE and AAE try to fit Gaussian distribution while preserving some geometric information but can't match Gaussian distribution absolutely. Due to the self drawbacks of GAN, the generated manifold using ALAE can not well preserve the geometry of data manifold. Although imposing reciprocity in the latent space gives some advantages to choosing measure metrics, they also can not preserve topological properties. Therefore, ALAE gets bad results for reconstruction. There is no trade-off problem with our approach. The latent embedding can fully preserve geometric information. With an adversarial strategy, we can obtain a satisfying latent distribution mapping to generate new data within original data manifold from a specified prior.

Ablation Study

We do an ablation study on Mnist dataset to verify each component of our framework including adversarial regularizer and batch normalization(BN). The latent dimension is set to 256D. We show the reconstructed, interpolated, and generated results with different combinations of each component. We can observe that all of the comparison methods can get well-performed reconstruction results. However, without BN for latent embedding, we fail to generate digital images. This is mainly because the embedding distribution may be overdispersed in 256-dimensional latent space which is dif-

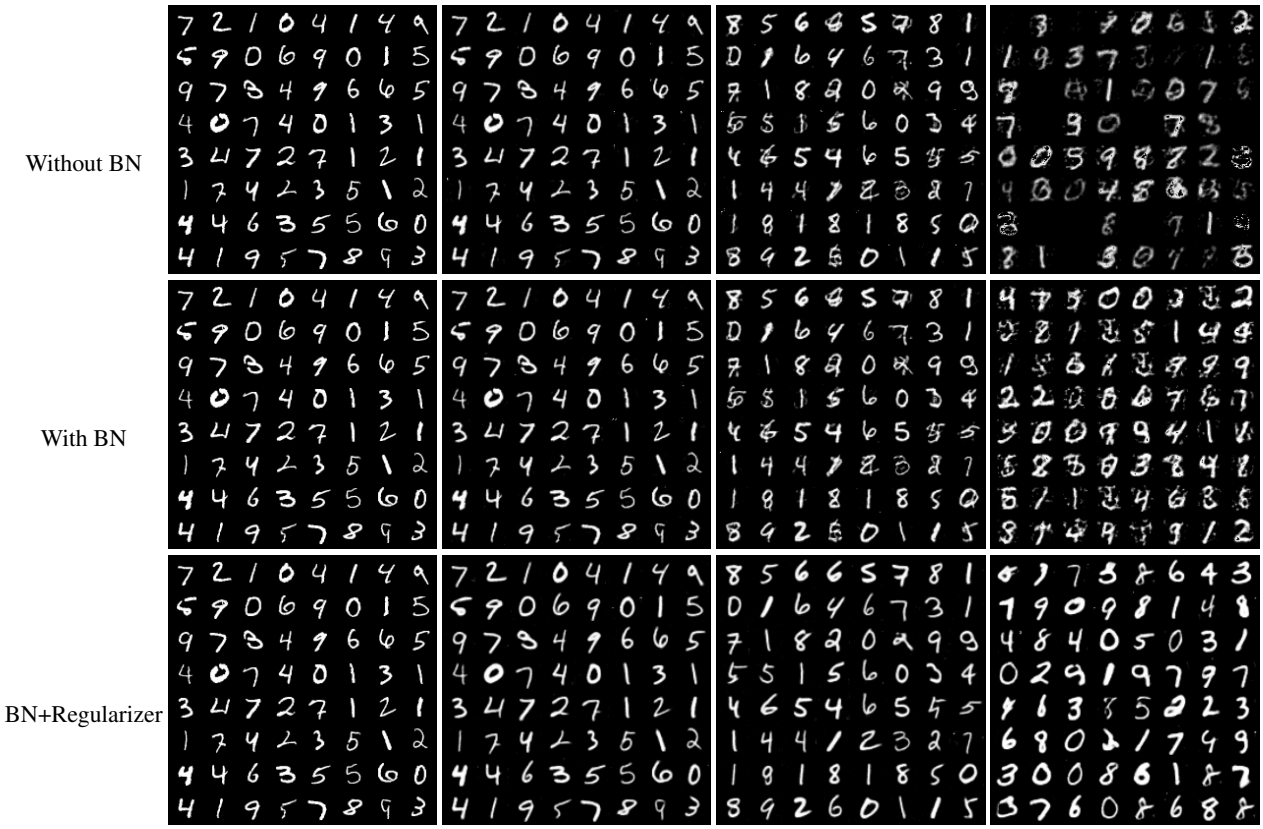

Figure 6: Results on MNIST Dataset. BN represents batch normalization operation.

ficult for the prior to learn. This also brings more challenges to interpolation tasks. With BN operation, the generated images have better visual quality but may have some overlaps by two digits. After adding our adversarial regularizer, we can generate sharp digital images with high quality, as well as interpolated results. This demonstrates our adversarial regularizer can further improve the learning ability aimed at latent distribution while BN makes the embedding subjected to a distribution with its mean close to 0 and variance close to 1.

CelebA Dataset

For CelebA datasets, we measure the performance quantitatively with FID scores [Heusel et al. 2017] for generated images and MSE metric for reconstructed images. FID can detect intra-class mode dropping, and measure the diversity as well as the quality of generated samples. All the training and testing images are resized to 64. FID is computed from 50K generated samples and the pre-calculated statistics are precomputed on all training data. The model architecture for networks G, g and D, d follow the Mimicry's architectures [Lee and Town 2020]. We compare our model with other autoencoder based methods including VAE [Kingma and Welling 2014], AAE [Makhzani et al. 2015], WAE [Tolstikhin et al. 2018], introVAE [Huang et al. 2018] and AGE [Ulyanov, Vedaldi, and Lempitsky 2017]. Each model is trained for 25 epochs. Table 1 shows the quantitative evaluation results. Our method obtains the best results both on FID and MSE, indicating that our method can achieve better performance both on reconstruction and generation rather than a trade-off between them. Moreover, we show the qualitative visual results for our approach and those comparison methods above in Fig. 7 and Fig. 8. We can observe our method produces visually appealing results both in reconstruction and sampling. Both the quantitative and qualitative results demonstrate our method is able to preserve the most global topology information of the input data manifold while achieving high-quality generation in visual perception.

Methods	VAE	AAE	WAE	IntroVAE	AGE	Ours
FID	80	101	115	120	116	62
MSE	0.0383	0.0255	0.0626	0.0562	0.0889	0.0165

Table 1: The FID and MSE values for different methods on CelebA Dataset.

Metrics	Datasets	VAE	AAE	WAE	IntroVAE	AGE	Ours
FID	cifar10	189	120	173	133	271	
	CelebA	80	101	115	120	116	63
MSE	cifar10	0.0626	0.0245	0.0607	0.0492	0.0608	
	CelebA	0.0383	0.0255	0.0626	0.0562	0.0889	0.0165

Table 2

Conclusion

Despite the recent success of variational autoencoder and its variants, there exists a trade-off between reconstruction and generation. Rather than imposing the latent distribution matching the prior, we propose to let the prior fit a learned latent representation which preserves the topological properties of the data manifold. In order to learn a latent distribution which is conducive to prior learning, we introduce an adversarial regularizer on interpolated samples and a batch normalization trick on latent embedding to obtain a concentrated latent distribution. We give a theoretical analysis of the superiority of our method and perform extensive experiments to further verify its effectiveness. Our experiments show that our method is able to preserve the most global topology information of the input data manifold while achieving high-quality generation without sampling meaningless points.

References

Berthelot, D.; Raffel, C.; Roy, A.; and Goodfellow, I. 2019. Understanding and Improving Interpolation in Autoencoders via an Adversarial Regularizer. In *Proceedings of the 7th International Conference on Learning Representations*.

Blum, A.; Hopcroft, J.; and Kannan, R. 2016. Foundations of data science. *Vorabversion eines Lehrbuchs* 5.

Bouchacourt, D.; Tomioka, R.; and Nowozin, S. 2017. Multi-Level Variational Autoencoder: Learning Disentangled Representations from Grouped Observations. *arXiv preprint arXiv:1705.08841* .

Brock, A.; Donahue, J.; and Simonyan, K. 2019. Large Scale GAN Training for High Fidelity Natural Image Synthesis. *Proceedings of the 2nd International Conference on Learning Representations* .

Davidson, T. R.; Falorsi, L.; De Cao, N.; Kipf, T.; and Tomczak, J. M. 2018. Hyperspherical variational auto-encoders. *arXiv preprint arXiv:1804.00891* .

Goodfellow, I. J.; Pouget-Abadie, J.; Mirza, M.; Xu, B.; Warde-Farley, D.; Ozair, S.; Courville, A.; and Bengio, Y. 2014. Generative Adversarial Networks. *Advances in Neural Information Processing Systems* 3: 2672–2680.

Heusel, M.; Ramsauer, H.; Unterthiner, T.; Nessler, B.; and Hochreiter, S. 2017. Gans trained by a two time-scale update rule converge to a local nash equilibrium. In *Advances in neural information processing systems*, 6626–6637.

Huang, H.; Li, Z.; He, R.; Sun, Z.; and Tan, T. 2018. IntroVAE: Introspective Variational Autoencoders for Photographic Image Synthesis. *Advances in Neural Information Processing Systems* .

Kingma, D. P.; and Welling, M. 2014. Auto-Encoding Variational Bayes. In *Proceedings of the 2nd International Conference on Learning Representations*.

Larsen, Anders Boesen Lindbo, S. K. S. H. L.; and Winther, O. 2016. Autoencoding beyond pixels using a learned similarity metric. *International conference on machine learning* .

LeCun, Y. 1998. The MNIST database of handwritten digits. *http://yann. lecun. com/exdb/mnist/* .

Lee, K. S.; and Town, C. 2020. Mimicry: Towards the Reproducibility of GAN Research .

Liu, Z.; Luo, P.; Wang, X.; and Tang, X. 2015. Deep learning face attributes in the wild. In *Proceedings of the IEEE international conference on computer vision*, 3730–3738.

Makhzani, A.; Shlens, J.; Jaitly, N.; and Goodfellow, I. 2015. Adversarial Autoencoders. *arXiv preprint arXiv:1511.05644* .

Mathieu, Emile, T. R. N. S.; and Teh, Y. W. 2019. Disentangling disentanglement in variational autoencoders. *International Conference on Machine Learning* .

Oord, A. V. D.; Vinyals, O.; and Kavukcuoglu, K. 2017. Neural Discrete Representation Learning. *Advances in Neural Information Processing Systems* .

Pidhorskyi, S.; Adjeroh, D. A.; and Doretto, G. 2020. Adversarial Latent Autoencoders. In *2020 IEEE/CVF Conference on Computer Vision and Pattern Recognition*. Seattle, WA, USA. ISBN 978-1-72817-168-5. doi:10.1109/CVPR42600.2020.01411.

Qian, S.; Li, G.; Cao, W. M.; Liu, C.; and Wong, H. S. 2019. Improving representation learning in autoencoders via multidimensional interpolation and dual regularizations. In *Twenty-Eighth International Joint Conference on Artificial Intelligence*.

Tolstikhin, I.; Bousquet, O.; Gelly, S.; and Schoelkopf, B. 2018. Wasserstein Auto-Encoders. *Proceedings of the 2nd International Conference on Learning Representations* .

Ulyanov, D.; Vedaldi, A.; and Lempitsky, V. 2017. It Takes (Only) Two: Adversarial Generator-Encoder Networks. *Proceedings of the AAAI Conference on Artificial Intelligence* .

van Handel, R. 2014. Probability in high dimension. Technical report, PRINCETON UNIV NJ.

Vincent, P.; Larochelle, H.; Lajoie, I.; Bengio, Y.; and Manzagol, P. A. 2010. Stacked Denoising Autoencoders: Learning Useful Representations in a Deep Network with a Local Denoising Criterion. *Journal of Machine Learning Research* 11(12): 3371–3408.

Xu, J.; and Durrett, G. 2018. Spherical Latent Spaces for Stable Variational Autoencoders. *Conference on Empirical Methods in Natural Language Processing* .

Zhang, H.; Goodfellow, I.; Metaxas, D.; and Odena, A. 2019. Self-Attention Generative Adversarial Networks. In *International Conference on Machine Learning*.

Zhao, D.; Zhu, J.; and Zhang, B. 2019. Latent Variables on Spheres for Autoencoders in High Dimensions. *arXiv* arXiv–1912.

Zhao, S.; Song, J.; and Ermon, S. 2019. Infovae: Balancing learning and inference in variational autoencoders. In *Proceedings of the aaai conference on artificial intelligence*, volume 33, 5885–5892.

(a) VAE (b) AAE (c) WAE

(d) IntroVAE (e) AGE (f) Ours

Figure 7: The generated results with different methods for CelebA Dataset.

(a) VAE (b) AAE (c) WAE (d) IntroVAE (e) AGE (f) Ours

Figure 8: The reconstructed results with different methods for CelebA Dataset.